The influence of diffusion on photoinduced electron transfer and geminate recombination

R. C. Dorfman and M. D. Fayer
Department of Chemistry, Stanford University, Stanford, California 94305

(Received 7 November 1991; accepted 5 February 1992)

The influence of diffusion on photoinduced electron transfer and geminate recombination in solutions of randomly distributed donors and acceptors is explored. The focus is on the effect diffusional motion has on geminate recombination. The reactive state (state following photoinduced electron transfer) probability is calculated as a function of diffusion constant and relative permittivity for three intermolecular potential cases: attractive, repulsive, and no Coulomb potentials. Also calculated are the reactive state yield and reactive state survival fraction. Both forward and back electron-transfer rates are distance dependent (not contact transfer). Any diffusion constant can be investigated, and donor–acceptor and acceptor–acceptor excluded volumes are taken into account. The model developed here is compared with slow and fast diffusion limits as well as with the theories of Smoluchowski, and Collins and Kimball.

I. INTRODUCTION

Photoinduced electron transfer from a neutral donor to a neutral acceptor (or cationic acceptor) in an ensemble of randomly distributed donors and acceptors generates a radical pair that are in close proximity. The ions and/or neutrals created by forward electron transfer are highly reactive and can go on to do useful chemistry. However, since the thermodynamically stable state of the pair is the original parent molecules, there is a strong tendency for electron back transfer to occur prior to ion separation by diffusion. The lifetime of photogenerated ions in solution depends on the forward and back electron-transfer parameters,[1] the concentration of donors and acceptors, the interaction potential between the ions, and on the diffusion[2–6] characteristics of the donor (D) and acceptor (A) (viscosity of the solvent). In this paper, we extend the theory of photoinduced electron transfer and back transfer in solid solutions[7,8] to include diffusion of the particles. This extends the theory to liquids and provides a comprehensive description of the competition between electron back transfer and separation by diffusion.

The importance of particle motion and its effects on chemical reactions cannot be understated. In batteries, the motion of charged particles through an electrolyte solution to eventual oxidation or reduction at an electrode is fundamental to its operation.[9] In chemical reactions in solution, molecules may react on contact with each other or at a distance (as in some electron transfer reactions).[7] Many biochemical charge-transfer reactions take place in fluid media whose properties govern life processes.[1] Before current can flow in a fuel cell, the fuel has to diffuse to an electrode for electron transfer to occur and the spent fuel must diffuse away. These diffusion processes can effect the current output and efficiency of the fuel cell.[10,11]

The nature and importance of diffusion in chemical systems has been studied for many years.[12–14] More recently, a considerable amount of work has been done on the influence of translational and rotational diffusion on excitation transport among molecules in liquids.[15–23] In these treatments, the assumption of a slow or fast diffusion process relative to the transfer time is assumed in order to make the mathematics more tractable. The influence of diffusion on electron transfer has also been studied both experimentally[24–27] and theoretically.[26,28–36] In these studies various assumptions have limited the general applicability of the theoretical results. In one study, the low concentration limit of acceptors was used to obtain information only on forward electron transfer.[28] In other studies, transfer is allowed only at contact between the donor and acceptor.[26,29,30,33,34] In a work by Mikhelashvili,[37,38] *et al.*, both forward and back transfer with donor–acceptor excluded volume was taken into account, but did not include the effects of acceptor–acceptor excluded volume. However, they use a different method for calculating the back transfer problem than the one in this work. A theoretical study[39] that compares several methods for analyzing the forward/back transfer problem has demonstrated that the method of Mikhelashvili *et al.* is accurate only at very low concentrations, concentrations that are not of experimental interest. Steady-state and time-resolved fluorescence experiments have been used to measure the effect of diffusion on forward electron transfer between the ions rhodamine B and ferrocyanide.[24] This study used a variety of models to analyze the experimental data. Consistent fits were not obtained with any of the models. In another experimental work,[25] the Smoluchowski equation modified with a distance dependent sink function was used to analyze data on forward electron transfer between neutral donors and neutral acceptors. This was more successful at analyzing the data.

Chemical reaction dynamics in liquids is a heavily studied area. It is well known that solvent properties such as viscosity[26] and dielectric constant[40–44] can effect chemical reactions between solute molecules. Other properties such as the relative size[43] of the solvent and solute play a role in

 0021-9606/92/107410-13$06.00

determining the dielectric properties and therefore the reaction dynamics. The solvent properties may not always be estimated from the bulk viscosity or dielectric constant. It has been demonstrated that the microscopic viscosity[26,45] and the microscopic dielectric properties[40,42–44] can be different from the bulk.

The interaction potential between reactants and products can be important. For neutral molecules, the force that one molecule exerts on another when not in contact is quite small. When a pair of molecules has like or opposite charges the situation is different. In low dielectric solvents the force between the molecules can be quite strong and have a dramatic effect on the reaction yield. In a solvent with a high dielectric constant the force between the molecules can be diminished to the point of being negligible.

In solid solution, at high concentrations of solute (reactant), one must account for the finite size of the molecules because they may fill a large portion of the sample volume.[7] In liquid solution, the effect of excluded volume might be different because two different molecules can now occupy the same space but with the condition that it be at different times. This suggests that there might be a time scale (or diffusion constant) during which excluded volume becomes less important than in solid solution. Certainly at very short times (or small diffusion constants), the molecules in liquids have barely moved from their initial positions and are represented by the solid solution result quite well. At long time the particle positions, relative to their initial positions, have randomized and their trajectories have overlapped.

In this work, we treat the problem of photoinduced electron transfer and geminate recombination for any diffusion constant, any acceptor concentration and size, any combination of forward and back electron-transfer parameters and various ionic interaction potentials (including different dielectric constants and attractive/repulsive/noninteracting potentials). The model presented here is for a three level system (see Fig. 1). We will call the various states the ground, excited, and reactive states. The model encompasses the three cases that are represented in Eqs. (1)–(3). Case I has as its excited state a neutral excited D^* molecule with a neutral A molecule. Its reactive state is an ion pair of opposite charges (D^+A^-), while the ground state is the neutral D and A. Case II is different, the A^{++} molecule (acceptor) has a $+2$ charge, the reactive state has like charges on the molecules (D^+A^+), and the ground state has the neutral D with the ground state A^{++}. Case III has an excited state composed of an excited neutral D^* with a positively charged A^+. The reactive state has a neutral A with a positively charged D^+, and the ground state has a neutral D with a positively charged A^+. These specific cases were chosen because there is no Coulomb interaction between the initial species. Therefore it is reasonable to assume that they are randomly distributed. The material presented below can be applied to nonrandom initial conditions by performing the appropriate spatial average. Transitions between the three states can occur via fluorescence from the excited state to the ground state or by forward electron transfer from the excited state to the reactive state and by back electron transfer from the reactive state to the ground state. The chemical reaction

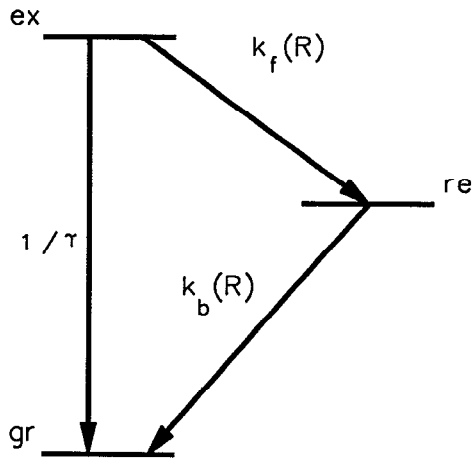

FIG. 1. Level diagram showing the three states: the ground (gr), excited (ex), and reactive (re) states. The three rate processes are represented by their rates τ, $k_f(R)$, and $k_b(R)$, which are the fluorescence lifetime of the donor, the forward, and back transfer rates, respectively. The three cases explored here are given in detail in Sec. I.

equations for these cases are given in Eqs. (1)–(3).

$$D+A \overset{k}{\leftarrow} D^* + A \overset{k_f}{\rightarrow} D^+ + A^- \overset{k_b}{\rightarrow} D+A, \tag{1}$$

$$D+A^{++} \overset{k}{\leftarrow} D^* + A^{++} \overset{k_f}{\rightarrow} D^+ + A^+ \overset{k_b}{\rightarrow} D+A^{++}, \tag{2}$$

$$D+A^+ \overset{k}{\leftarrow} D^* + A^+ \overset{k_f}{\rightarrow} D^+ + A \overset{k_b}{\rightarrow} D+A^+. \tag{3}$$

The relevant rate constants are given in Eqs. (4)–(6).

$$k = \frac{1}{\tau}, \tag{4}$$

$$k_f(R) = \frac{1}{\tau}\exp[(R_f - R)/a_f], \tag{5}$$

$$k_b(R) = \frac{1}{\tau}\exp[(R_b - R)/a_b]. \tag{6}$$

In Eqs. (4)–(6), τ is the fluorescence lifetime of D's excited state, $k_f(R)$ is the forward electron-transfer rate, $k_b(R)$ is the back electron-transfer rate, R is the D–A separation, and a_f, a_b, R_f, R_b are parameters that characterize the falloff of the donor–acceptor wave function overlap.[1,7] These rates assume that the electron transfer is in the nonadiabatic limit.[1] This is a common assumption for intermolecular electron transfer. This model is not limited to this form of the electron-transfer rate. In fact, any form for the electron-transfer rate can be used as long as it is time independent. In all cases, we will call the D molecule the donor and the A molecule the acceptor. Of course, when back transfer occurs their roles are reversed.

In Sec. II, the fundamental equations that describe the evolution of the three states will be derived. In Sec. III, calculations for the excited (which is proportional to the time dependent fluorescence observable) and reactive state populations, the reactive state distribution function, the fluores-

cence yield, and the pump–probe observable for the three cases with a variety of parameters will be presented.

II. ELECTRON TRANSFER AND BACK TRANSFER IN SOLUTION

In this section we will derive the excited state ($\langle P_{ex}(t)\rangle$), and reactive state ($\langle P_{re}(t)\rangle$) populations. We start by determining the probabilities of finding the donor molecule in its excited or reactive state for a system containing only two molecules, the donor D and the acceptor A in solution.

In the problem presented here the initial condition is donors in their excited states at $t=0$. Each donor is surrounded by a random distribution of acceptors. As time progresses probability will flow out from the donor to the acceptors. The probability that a particular excited donor is still in the excited state is a function of time and acceptor position. Donors and acceptors that are close interact more strongly than those further apart. The function that describes the survival of an excited donor is called the excited state survival probability. This survival probability also governs the rate of reactive state formation (for example, an ion pair as in case I presented earlier). Since the excited state survival probability is a function of both time and distance and the acceptors are randomly distributed, the reactive states will be formed over a distribution of times and distances. Once the reactive state has been formed recombination can occur, returning the system to the ground state. The survival of the reactive state pair is now governed by the reactive state survival probability. The reactive state survival probability describes the survival of the reactive state and its loss due to back transfer to the ground state; it does not contain a source term. Since the reactive states are formed over a distribution of times and distances, the reactive state population is obtained by convolving the rate of reactive state formation (which is a function of the excited state population, the excited state survival probability and the forward transfer rate) with the reactive state survival probability. The reactive state survival probability is calculated for all pairs created at a single time. The function describing the reactive state survival probability is then convolved with the function that describes reactive state formation. The convolution yields the appropriate reactive state population function.

The method of convolving a survival probability (Green's function) with the appropriate source term is used in many fields. It has been employed previously in electron-transfer and diffusion problems.[26,28,32–38] The survival probabilities that will be derived in the next section are used to obtain populations and related observables.

In the model the donor has only one accessible electronic excited state, and the acceptor has one acceptor state. All three states have the same multiplicity, e.g., singlets. The concentration of the donor molecule is low enough that excitation migration among the donor molecules does not occur and that the back transfer is geminate. The electron-transfer rates [see Eqs. (4)–(6)] are exponentially decaying functions of the donor–acceptor separation. Acceptor–acceptor transfer is not allowed because the energetics highly favor back transfer.

A. One donor and one acceptor

At $t=0$, the donor is optically excited. In the absence of the acceptor, the probability of finding the donor excited decays exponentially with the excited state life time, τ, where $\langle P_{ex}(t)\rangle = \exp(-t/\tau)$. When an acceptor is present, the probability decreases more rapidly due to the addition of the electron-transfer pathway to the acceptor.

The survival probabilities of the excited, $S_{ex}(R,t)$, and reactive states, $S_{re}(R,t)$, for solid solution[7,32,39] are given by the following equations for one acceptor in the absence of fluorescence:

$$S_{ex}(R,t) = \exp[-k_f(R)t], \tag{7}$$

$$S_{re}(R,t) = \exp[-k_b(R)t]. \tag{8}$$

These are the probabilities that the state (excited or reactive) will still survive after a time t with a donor–acceptor separation of R in the absence of fluorescence. To include fluorescence one multiplies the survival probability by $\exp(-t/\tau)$.

In liquid solution, the situation is more complicated because the positions of the particles are not static. The donor and acceptor molecules undergo diffusive motion characterized by their corresponding diffusion constants D_D and D_A. It is convenient to describe the position of the acceptor in a reference frame whose origin coincides at any instant with the center of mass of the donor. In this reference frame the acceptor undergoes diffusive motion relative to a stationary donor characterized by the diffusion constant $D = D_D + D_A$.[6,19,26,34] For the three cases introduced earlier, there are no significant intermolecular forces between the donor and acceptor prior to electron transfer. This means that the donors and the acceptors are randomly distributed and are freely diffusing. To obtain the survival probability for the excited state we start with the following Green's function:[26,33]

$$\frac{\partial}{\partial t} G_{ex}(R,t|R_0) = D\nabla_R^2 G_{ex}(R,t|R_0) - k_f(R) G_{ex}(R,t|R_0), \tag{9}$$

$$G_{ex}(R,0|R_0) = \frac{\delta(R-R_0)}{4\pi R_0^2}, \tag{10}$$

$$4\pi R_m^2 D \frac{\partial}{\partial R} G_{ex}(R,t|R_0)\Big|_{R=R_m} = 0, \tag{11}$$

where in Eq. (9) $G_{ex}(R,t|R_0)$ represents the probability distribution of the excited state at a time t, if at $t=0$ the separation is R_0. ∇_R^2 for the spherically symmetric case considered here is

$$\nabla_R^2 = \frac{2}{R}\frac{\partial}{\partial R} + \frac{\partial^2}{\partial R^2}. \tag{12}$$

The first term in Eq. (9) accounts for the diffusional motion of the particles and the second term is a sink due to electron transfer. The initial condition is given in Eq. (10). At $t=0$ the donor is excited and the acceptor is at its initial position. We use a reflecting boundary condition which is given by Eq. (11) (the particle flux through the boundary is zero). This can be important because the electron-transfer rate is finite

at contact. Therefore, the donor and the acceptor can contact and diffuse apart without undergoing electron transfer.

The reactive state has a Green's function associated with its probability distribution function given by the following equation:[26,33]

$$\frac{\partial}{\partial t} G_{re}(R,t|R_0) = L_R G_{re}(R,t|R_0) - k_b(R) G_{re}(R,t|R_0), \tag{13}$$

$$G_{re}(R,0|R_0) = \frac{\delta(R-R_0)}{4\pi R_0^2}, \tag{14}$$

$$4\pi R_m^2 D \exp[-V(R)] \frac{\partial}{\partial R} \times \exp[V(R)] G_{re}(R,t|R_0)\Big|_{R=R_m} = 0, \tag{15}$$

where L_R is the Smoluchowski operator given by[26,33]

$$L_R = \frac{1}{R^2}\frac{\partial}{\partial R} D R^2 \exp[-V(R)] \frac{\partial}{\partial R} \exp[V(R)]. \tag{16}$$

$V(R)$ is the interaction potential between the donor and the acceptor in the reactive state divided by $K_B T$. Here $V(R)$ is a Coulomb potential and is given by

$$V(R) = \left(\frac{Z_D Z_A e^2}{4\pi\epsilon_0 \epsilon_r K_B T}\right)\frac{1}{R}$$

where Z_D and Z_A are the numbers and signs of the charges on the donor and the acceptor, respectively, e is the charge of the electron, ϵ_0 is the permittivity of free space, ϵ_r is the relative permittivity of the solvent, K_B is Boltzmann's constant, and T is the temperature.

In all cases, the donor–acceptor pairs start at some location at $t = 0$, then diffuse. Since the sink functions (the electron-transfer rates) extend over space, and are not just at contact, electron transfer will happen concurrently with diffusion. If the pair separation is initially very large then the particles will undergo essentially free diffusion until they come into the range of forward electron transfer for the excited state and the range of the interaction potential and back transfer for the reactive state. If the pair separation is initially small then the particle motion and survival probability may depend mostly on the nature of the interaction potential and the electron transfer rate.

To obtain the survival probabilities one takes the adjoints of Eqs. (9)–(16) and then integrates over R.[26,33] The purpose of taking the adjoints is that it allows for analytical integration over the R coordinate, which gives the pair survival probability. The adjoint equations are

$$\frac{\partial}{\partial t} G_{ex}(R,t|R_0) = D\nabla^2_{R_0} G_{ex}(R,t|R_0) - k_f(R_0) G_{ex}(R,t|R_0), \tag{17}$$

$$G_{ex}(R,0|R_0) = \frac{\delta(R-R_0)}{4\pi R^2}, \tag{18}$$

$$4\pi R_m^2 D \frac{\partial}{\partial R_0} G_{re}(R,t|R_0)\Big|_{R_0=R_m} = 0, \tag{19}$$

$$\frac{\partial}{\partial t} G_{re}(R,t|R_0) = L^\dagger_{R_0} G_{re}(R,t|R_0) - k_b(R_0) G_{re}(R,t|R_0), \tag{20}$$

$$G_{re}(R,0|R_0) = \frac{\delta(R-R_0)}{4\pi R^2}, \tag{21}$$

$$4\pi R_m^2 D \frac{\partial}{\partial R_0} G_{re}(R,t|R_0)\Big|_{R_0=R_m} = 0, \tag{22}$$

where $\nabla^2_{R_0}$ is given by Eq. (12) with R replaced by R_0 and $L^\dagger_{R_0}$ is given by[26,33]

$$L^\dagger_{R_0} = \frac{1}{R_0^2}\exp[V(R_0)]\frac{\partial}{\partial R_0} D R_0^2 \exp[-V(R_0)]\frac{\partial}{\partial R_0}. \tag{23}$$

In the adjoint equations, the operators are now functions of R_0 and both sides may be integrated over R to give the the survival probabilities:

$$\frac{\partial}{\partial t} S_{ex}(t|R_0) = D\nabla^2_{R_0} S_{ex}(t|R_0) - k_f(R_0) S_{ex}(t|R_0), \tag{24}$$

$$S_{ex}(0|R_0) = 1, \tag{25}$$

$$4\pi R_m^2 D \frac{\partial}{\partial R_0} S_{ex}(t|R_0)\Big|_{R_0=R_m} = 0, \tag{26}$$

$$\frac{\partial}{\partial t} S_{re}(t|R_0) = L^\dagger_{R_0} S_{re}(t|R_0) - k_b(R_0) S_{re}(t|R_0), \tag{27}$$

$$S_{re}(0|R_0) = 1, \tag{28}$$

$$4\pi R_m^2 D \frac{\partial}{\partial R_0} S_{re}(t|R_0)\Big|_{R_0=R_m} = 0. \tag{29}$$

Equations (24) and (27) for the excited- and reactive state survival probabilities, respectively, cannot be solved analytically. There are, however, analytical solutions for very small[35] and very large diffusion constants[36] as well as solutions for transfer only at contact.[26,33] Here the survival probabilities will be solved numerically since the diffusion constants explored in this work are intermediate between the small and large diffusion limits and electron transfer occurs over a range of distances with a distance dependent rate.

B. A donor and many acceptors

The partial differential equations describing electron transfer with diffusion for a donor and N acceptors having an initial configuration of R_{0_j} ($j = 1,...,N$) and a configuration of R_j ($j = 1,...,N$) at a time t are given in the following for an infinitely long excited-state fluorescence lifetime:

$$\frac{\partial}{\partial t} P_{ex}(R_1,...,R_N,t|R_{01},...,R_{0N}) = \sum_{j=1}^{N} [D\nabla_j^2 - k_f(R_j)] P_{ex}(R_1,...,R_N,t|R_{01},...,R_{0N}), \tag{30}$$

$$P_{ex}(R_1,...,R_N,0|R_{01},...,R_{0N}) = \prod_{j=1}^{N} \frac{\delta(R_j - R_{0j})}{4\pi R_{0j}^2}, \tag{31}$$

$$4\pi R_m^2 D \frac{\partial}{\partial R_j} P_{re}(R_1,...,R_N,t|R_{01},...,R_{0N})\Big|_{R_j=R_m} = 0 \quad (j=1,...,N), \tag{32}$$

$$\frac{\partial}{\partial t} P_{re}^i(R_1,...,R_N,t|R_{01},...,R_{0N}) = \sum_{j=1}^{N} L_{R_j} P_{re}^i(R_1,...,R_N,t|R_{01},...,R_{0N}) - k_b(R_i) P_{re}^i(R_1,...,R_N,t|R_{01},...,R_{0N}) + k_f(R_i) P_{ex}(R_1,...,R_N,t|R_{01},...,R_{0N}) \quad (i=1,...,N), \tag{33}$$

$$P_{re}^i(R_1,...,R_N,0|R_{01},...,R_{0N}) = 0 \quad (i=1,...,N), \tag{34}$$

$$4\pi R_m^2 D \exp[-V(R_j)] \frac{\partial}{\partial R_j} \exp[V(R_j)] \times P_{re}(R_1,...,R_N,t|R_{01},...,R_{0N})|_{R_j=R_m} = 0 \quad (j=1,...,N), \tag{35}$$

where $P_{ex}(R_1,...,R_N,t|R_{01},...,R_{0N})$ is the excited-state probability with the initial condition given by Eq. (31) and boundary condition given by Eq. (32). $P_{re}^i(R_1,...,R_N,t|R_{01},...,R_{0N})$ is the probability that the system is in the reactive state and the ith acceptor has the electron. The initial condition is given by Eq. (34) and the boundary condition is given by Eq. (35). This is only exact in the limit of $D_D = 0$, but is a very accurate approximation in three-dimensional systems.[34]

The solution of Eq. (30) is given by[32]

$$P_{ex}(R_1,...,R_N,t|R_{01},...,R_{0N}) = \prod_{j=0}^{N} G_{ex}(R_j,t|R_{0j}), \tag{36}$$

where $G_{ex}(R_j,t|R_{0j})$ is the solution to Eq. (17). The survival probability is then obtained by integrating over all R:

$$P_{ex}(t|R_{01},...,R_{0N}) = \prod_{j=0}^{N} S_{ex}(t|R_{0j}), \tag{37}$$

where $S_{ex}(t|R_{0j})$ is the one acceptor survival probability given in Eq. (24). The ensemble averaged excited-state population in the thermodynamic limit has been derived for point particles and donor–acceptor excluded volume[7,32,46] and is given by

$$\langle P_{ex}(t)\rangle = \exp(-t/\tau) \times \exp\left(-4\pi C \int_{R_m}^{\infty} [1 - S_{ex}(t|R_0)] R_0^2 dR_0\right), \tag{38}$$

where $\exp(-t/\tau)$ has now been added to account for the finite fluorescence lifetime of the excited state and R_m is the center-to-center distance of the donor and acceptor when they are in contact. This can also be written in terms of a time-dependent rate:[26]

$$\langle P_{ex}(t)\rangle = \exp(-t/\tau) \exp\left(-C \int_0^t k(t')dt'\right) \tag{39}$$

with $k(t)$ given by

$$k(t) = 4\pi \int_{R_m}^{\infty} k_f(R_0) S_{ex}(t|R_0) R_0^2 dR_0. \tag{40}$$

The inclusion of acceptor–acceptor excluded volume has also been done[7,47,48] and is given by

$$\langle P_{ex}(t)\rangle = \exp(-t/\tau)\exp\left(-\frac{4\pi}{d^3}\sum_{k=1}^{\infty}\frac{p^k}{k} \times \int_{R_m}^{\infty} [1 - S_{ex}(t|R_0)]^k R_0^2 dR_0\right), \tag{41}$$

where d is the acceptor diameter, $p = Cd^3$, and C is the concentration of acceptors in number density units. In this work, we will use the following expression which is equivalent to Eq. (41) because the sum in the exponential has a closed form:

$$\langle P_{ex}(t)\rangle = \exp(-t/\tau)\exp\left(\frac{4\pi}{d^3}\int_{R_m}^{\infty} \ln[1 - p + pS_{ex}(t|R_0)] R_0^2 dR_0\right). \tag{42}$$

This can also be written in terms of a time-dependent rate, which is given by

$$k(t) = 4\pi \int_{R_m}^{\infty} \left(\frac{1}{1 - p + pS(t|R_0)}\right) \times \left(-\frac{\partial S_{ex}(t|R_0)}{\partial t}\right) R_0^2 dR_0. \tag{43}$$

This substituted into Eq. (39) will give the excited-state population. In the limit that d, the acceptor excluded volume, goes to zero, Eq. (43) goes to Eq. (40), the result with only donor–acceptor excluded volume. Substitution for the time derivative with Eq. (24) gives the more explicit form

$$k(t) = 4\pi \int_{R_m}^{\infty} \left(\frac{k_f(R_0) S_{ex}(t|R_0)}{1 - p + pS_{ex}(t|R_0)}\right) R_0^2 dR_0 - 4\pi \int_{R_m}^{\infty} \left(\frac{D\nabla_{R_0}^2 S_{ex}(t|R_0)}{1 - p + pS_{ex}(t|R_0)}\right) R_0^2 dR_0. \tag{44}$$

In the case of no acceptor–acceptor excluded volume ($d = 0$), the second term goes to zero.

To get the ensemble averaged reactive state population, $\langle P_{re}(t)\rangle$, Eq. (33) is integrated over all R_j ($i = 1,...,N$) except R_i. The integration is defined as

$$P_{re}^i(R_i,t|R_{01},...,R_{0N}) = \left(\prod_{j\neq i}^{N} 4\pi \int_{R_m}^{R_V} R_j^2 dR_j\right) P_{re}^i(R_i,...,R_N,t|R_{01},...,R_{0N}), \tag{45}$$

and where the following is from the boundary condition,

$$\left(\prod_{j\neq i}^{N} 4\pi \int_{R_m}^{R_V} R_j^2 dR_j\right) \sum_{j\neq i}^{N} L_{R_j} P_{re}^i(R_i,...,R_N,t|R_{01},...,R_{0N}) = 0, \tag{46}$$

one gets

$$\frac{\partial}{\partial t} P_{re}^i(R_i,t|R_{01},...,R_{0N}) = L_{R_i} P_{re}^i(R_i,t|R_{01},...,R_{0N}) - k_b(R_i) P_{re}^i(R_i,t|R_{01},...,R_{0N})$$

$$+ k_f(R_i)\exp(-t/\tau)G_{ex}(R_i,t|R_{0i})\prod_{j\neq i}^{N}S_{ex}(t|R_{0j})$$
$$(i=1,...,N), \quad (47)$$

where the $\exp(-t/\tau)$ factor was added to the source term to account for loss of the excited state due to fluorescence. Averaging Eq. (47) over all R_0 except the ith one [average is similar to the integration defined in Eq. (45) except the time-dependent positions have been replaced with the initial positions and a factor of $1/V$ has been added, which is the volume occupied by the N acceptors ($V=4\pi R_V^3/3$)] gives

$$\frac{\partial}{\partial t}P^i_{re}(R_i,t|R_{0i}) = L_{R_i}P^i_{re}(R_i,t|R_{0i}) - k_b(R_i)P^i_{re}(R_i,t|R_{0i}) + k_f(R_i)G_{ex}(R_i,t|R_{0i})\langle P_{ex}(t)\rangle \quad (i=1,...,N). \quad (48)$$

In Eq. (48) $G_{ex}(R_i,t|R_{0i})$ is the solution to Eq. (13) and $\langle P_{ex}(t)\rangle$ is the excited-state population from Eq. (38). Equation (48) averaged over R_{0i} gives (after dropping the subscripts and superscripts) the reactive state distribution function[7]

$$\frac{\partial}{\partial t}P_{re}(R,t) = L_R P_{re}(R,t) - k_b(R)P_{re}(R,t) + \frac{1}{V}k_f(R)S_{ex}(t|R)\langle P_{ex}(t)\rangle. \quad (49)$$

In Eq. (49) the factor $S_{ex}(t|R)$ comes from the fact that Eqs. (9) and (17) are self-adjoint, which means that integrating Eq. (9) over R_0 or Eq. (17) over R gives the same function only with R as the variable in Eq. (9) and R_0 in Eq. (17). This is not true for the reactive state survival probability. The operators L_R and $L^{\dagger}_{R_0}$ are different operators and are not converted to the other upon interchanging R and R_0.

The initial condition for Eq. (49) is obtained by integrating Eq. (33) over all spatial coordinates except R:

$$P_{re}(R,0) = 0. \quad (50)$$

The boundary condition is reflecting

$$4\pi R_m^2 D\exp[-V(R)]\frac{\partial}{\partial R}\exp[V(R)]P_{re}(R,t)\Big|_{R=R_m} = 0. \quad (51)$$

The ensemble averaged reactive state probability is obtained by taking the solution of Eq. (49) and summing it over all the acceptors and then integrating over the last spatial coordinate. Since this term is the same for all the acceptors one gets [and with the factor $1/V$ removed from the last term in Eq. (49)]

$$\langle P_{re}(t)\rangle_{N,V} = \frac{4\pi N}{V}\int_{R_m}^{\infty}P_{re}(R,t)R^2dR. \quad (52)$$

In the thermodynamic limit the ratio N/V becomes the concentration C. Thus, the reactive state population is

$$\langle P_{re}(t)\rangle = 4\pi C\int_{R_m}^{\infty}P_{re}(R,t)R^2dR. \quad (53)$$

It is possible to write an analytical solution for the partial differential equation for the reactive state distribution function [Eq. (49)] in terms of the Green's function for the reactive state [Eq. (13)], the survival probability for the excited state [Eq. (24)], the ensemble averaged excited-state population [Eq. (38)], and the forward transfer rate [Eq. (5)]:

$$P_{re}(R,t) = \frac{1}{V}\int_0^t\int_{R_m}^{\infty}G_{re}(R,t-t'|R_0)k_f(R_0)S_{ex}(t'|R_0)\times\langle P_{ex}(t')\rangle 4\pi R_0^2dR_0dt'. \quad (54)$$

Taking the derivative of this with respect to t will give Eq. (49), proving this is a solution (in the thermodynamic limit the term $1/V$ is replaced by C). Also letting the diffusion constant $D=0$ gives the exact solid solution result, which has been derived elsewhere.[7] To get the total reactive state probability from this, it is integrated over the final coordinate and, in the thermodynamic limit, is

$$\langle P_{re}(t)\rangle = \int_0^t\int_{R_m}^{\infty}\left(\int_{R_m}^{\infty}4\pi CG_{re}(R,t-t'|R_0)R^2dR\right)\times k_f(R_0)S_{ex}(t'|R_0)\langle P_{ex}(t')\rangle 4\pi R_0^2dR_0dt'. \quad (55)$$

Since integrating the Green's function over R gives the survival probability for the reactive state [Eq. (27)] the final form for the reactive state population is

$$\langle P_{re}(t)\rangle = 4\pi C\int_{R_m}^{\infty}\int_0^t S_{re}(t-t'|R_0)k_f(R_0)S_{ex}(t'|R_0)\times\langle P_{ex}(t')\rangle dt'R_0^2dR_0. \quad (56)$$

This is an interesting result because it has the same form as the solid solution result[7] except the survival probabilities from Eqs. (24) and (27) with diffusion are used instead of the solid solution results given in Eqs. (7) and (8) and the excited-state population is calculated using Eq. (24) instead of Eq. (7).

Equation 56 for the reactive state population and Eqs. (49) and (54) for the reactive state distribution function only take into account donor–acceptor excluded volume. To account for acceptor–acceptor excluded volume the source term in Eq. (49) needs to be modified.[7,47–49] The differential equation for the reactive state distribution function becomes

$$\frac{\partial}{\partial t}P_{re}(R,t) = L_R P_{re}(R,t) - k_b(R)P_{re}(R,t) + \frac{1}{V}\left(\frac{1}{1-p+pS_{ex}(t|R)}\right)\times\left(-\frac{\partial S_{ex}(t|R)}{\partial t}\right)\langle P_{ex}(t)\rangle, \quad (57)$$

where the excited-state population is now given by Eq. (42). With this modification the solution becomes

$$P_{re}(R,t) = \frac{1}{V}\int_0^t\int_{R_m}^{\infty}\frac{G_{re}(R,t-t'|R_0)\langle P_{ex}(t')\rangle}{1-p+pS_{ex}(t'|R_0)}\times\left(-\frac{\partial S_{ex}(t'|R_0)}{\partial t'}\right)4\pi R_0^2dR_0dt' \quad (58)$$

(where in the thermodynamic limit $1/V$ is replaced by C) and the final result for the reactive state population is

$$\langle P_{re}(t)\rangle = 4\pi C \int_{R_m}^{\infty}\int_0^t \frac{S_{re}(t-t'|R_0)\langle P_{ex}(t')\rangle}{1-p+pS_{ex}(t'|R_0)} \times\left(-\frac{\partial S_{ex}(t'|R_0)}{\partial t'}\right) dt' R_0^2 dR_0, \quad (59)$$

where $\langle P_{ex}(t)\rangle$ is given by Eq. (42).

The probability that the system is found in any one of the three states, ground ($\langle P_{gr}(t)\rangle$), excited ($\langle P_{ex}(t)\rangle$), or the reactive ($\langle P_{re}(t)\rangle$) state is unity. Therefore, the ground-state population is

$$\langle P_{gr}(t)\rangle = 1 - \langle P_{ex}(t)\rangle - \langle P_{re}(t)\rangle. \quad (60)$$

In this section, the excited state [Eq. (42)], $\langle P_{ex}(t)\rangle$, and the reactive state [Eq. (59)], $\langle P_{re}(t)\rangle$ population functions have been derived. In Sec. III we will use these results as well as the ion distribution function in Eq. (58) to illustrate the detailed nature of the model as well as calculate the pump–probe experimental observable.

III. RESULTS AND DISCUSSION

In this section the excited-state [Eq. (42)] and reactive state [Eq. (59)] population functions will be displayed for a variety of parameters. The reactive state distribution function [eq. (58)] and some experimental observables will also be calculated. The partial differential equations for the survival probabilities were solved numerically. The formal treatment presented in Sec. II performed some of the necessary averaging analytically. It also formulated the problem in a manner amenable to numerical analysis. The Crank–Nicholson method[50] was used to solve these differential equations and Gaussian quadrature[50] was used for numerical integration. In each case, great care was exercised to ensure the accuracy of the numerical procedures. It was necessary to choose small enough distance and time steps to get stable and accurate solutions. The choice of the step sizes depend on the choice of parameters used. Typically, a distance step of 0.1 Å and time steps as small as 0.0001 ns were used and gave solutions that converged in a few minutes using a DEC3100 work station. For parameters that give faster dynamics, smaller step sizes are necessary. However, there is another numerical method for solving the partial differential equations that converges faster with larger step sizes,[35,51] which can be used in these cases.

A. Excited-state population $\langle P_{ex}(t)\rangle$

The excited-state population is displayed in Fig. 2 as a function of time, concentration, and diffusion constant. The diffusion constants used were 0, 0.1, 1, 10, 100, and ∞ Å^2/ns. For $D=0$, Eq. (42) was used with the solid solution result for the survival probability given in Eq. (7), and for $D=0.1$, 1, 10, and 100 Å^2/ns the solution to Eq. (24) was used in Eq. (42). The case with $D=\infty$ is given by[36]

$$\langle P_{ex}(t)\rangle = \exp(-t/\tau)\exp(-C\langle k\rangle t), \quad (61)$$

where

$$\langle k\rangle = 4\pi\int_{R_m}^{\infty} k_f(R)R^2 dR. \quad (62)$$

This follows from Eq. (44). In the limit that the diffusion constant goes to infinity, the survival probability $S_{ex}(t|R_0)$ goes to 1. The second term in Eq. (44) goes to zero and the first term gives Eq. (62). The concentrations used are $C=0.01$, 0.3, and 1 M of acceptor. The other parameters are $a_f=1$ Å, $R_f=12$ Å, $\tau=20$ ns, $R_m=9$ Å, and $d=7.2$ Å. These parameters were chosen because they are typical values. The values for R_m and d are for the rubrene/duroquinone system.[25] As can be seen, at each concentration the zero and infinite diffusion cases bracket the finite diffusion cases. There are analytical solutions for the small[35] and large[36] diffusion constant limits. For the parameters used in Fig. 2, the $D=0.1$ Å^2/ns is in the small diffusion limit and the $D=100$ Å^2/ns is in the large diffusion limit. The results agree well with the analytical results for these limiting cases. As is shown in Fig. 2 the excited-state population decreases more rapidly at higher acceptor concentrations and higher diffusion constants. When the diffusion constant is large enough the reaction rate is limited by the magnitude of the electron-transfer parameters.

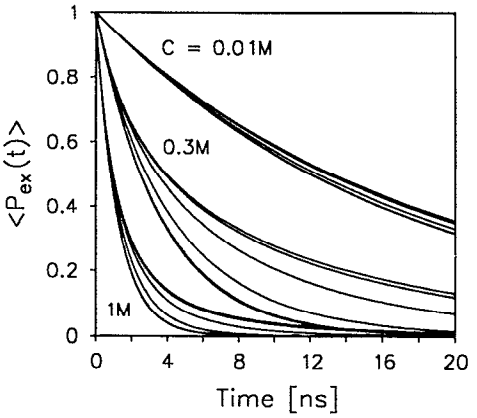

FIG. 2. Excited-state population probability as a function of time, concentration, and diffusion constant. The parameters used are $\tau=20$ ns, $R_f=12$ Å, $a_f=1$ Å, $R_m=9$ Å, and $d=7.2$ Å. The curves have concentrations $C=0.01$, 0.3, and 1 M, respectively. In each group of curves the diffusion constant ranged from $D=0$, 0.1, 1, 10, 100, and ∞ Å^2/ns. The upper curve in each group has $D=0$ and the bottom one has $D=\infty$. The other curves fall in between these two limits.

There are simpler models for diffusion influenced forward electron transfer; one is the Smoluchowski model.[26] In this model, the reaction is completely diffusion limited and reaction occurs instantly (infinite reaction rate) upon collision of the donor and the acceptor and does not occur otherwise. According to this theory the excited-state population is[26]

$$\langle P_{ex}(t)\rangle = \exp(-t/\tau) \times\exp\left[-4\pi R_m DC\left(1+\frac{2R_m}{(\pi Dt)^{1/2}}\right)t\right]. \quad (63)$$

Substituting values $R_m=9$ and the diffusion constants used in Fig. 2, Eq. (63) does not come close to giving the correct excited-state populations. It is possible to adjust the parameters D and R_m in Eq. (61) to attempt to fit the curves in Fig.

2. Adjusting the diffusion constant with $R_m = 9$ does not fit any of the curves in Fig. 2. Adjusting R_m while keeping D constant was only able to fit the $D = 100$ Å^2/ns curves with an $R_m = 0.95$, which is much smaller than the contact distance. The other curves could not be fit. Clearly, this shows that a distance dependent reaction is quite different from a diffusion limited contact reaction.

A more sophisticated theory is the Collins and Kimball model.[26] This is similar to the Smoluchowski theory except there is now a finite reaction rate (k) when the donor and the acceptor collide. Their result is[26]

$$\langle P_{ex}(t)\rangle = \exp(-t/\tau)\exp[-Cf(t)], \tag{64}$$

where

$$f(t) = \frac{4\pi DR_m k}{4\pi DR_m + k}\left(t + \frac{k}{4\pi D^2 R_m \alpha^2}\left[\exp(\alpha^2 Dt)\times\operatorname{erfc}(\alpha\sqrt{Dt}) + (2\alpha\sqrt{Dt}/\sqrt{\pi}) - 1\right]\right) \tag{65}$$

and

$$\alpha = \frac{4\pi DR_m + k}{4\pi DR_m^2}. \tag{66}$$

This theory is better at fitting the curves in Fig. 2. Using the diffusion constants and the R_m used to calculate the curves in Fig. 2 and only adjusting k, the transfer rate at contact, the $D = 10$, and 100 Å^2/ns curves were able to be fit. The fit values for k were 1550 Å^3/ns and 1350 Å^3/ns for the $D = 10$ Å^2/ns and $D = 100$ Å^2/ns cases, respectively. The smaller diffusion constants were not able to be fit. Although it was possible to fit two different diffusion constants with this model, they still did not give a single set of reaction rate parameters that fit all the curves. Thus, for reactions with distance dependent sinks, Eq. (24) must be used for the survival probability. An attempt to fit data with simpler models over a range of diffusion constants will not give a consistent set of parameters.

Calculations show that increasing the diffusion constant has the effect of eliminating the effect of acceptor–acceptor excluded volume. In solid solution, the particle positions are fixed and on the time scale for electron transfer no two particles can have overlapping volumes. In liquid solution, for large diffusion constants, the particle positions are changing rapidly on the time scale of electron transfer. Since the motions of the molecules are so fast, two molecules may occupy the same volume of space, at different times, but that exchange time is less than the time for reaction. Donor–acceptor excluded volume is important at all diffusion constants since it determines the maximum transfer rate.

B. Reactive state probability $\langle P_{re}(t)\rangle$

The reactive state probability is presented in Figs. 3–11 for various parameters and for the three cases mentioned in Sec. I. In Fig. 3 the reactive state yield is presented as a function of diffusion constant. The reactive state yield, ϕ_{re}, can be calculated from the relative fluorescence yield:

$$\phi_{re} = 1 - \phi_{ex}, \tag{67}$$

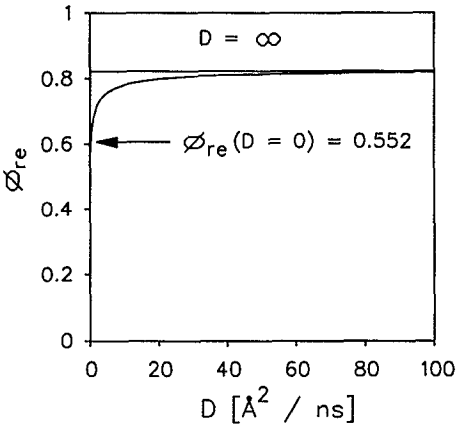

FIG. 3. Reactive state yield versus the diffusion constant. The yield increases rapidly to about 20 Å^2/ns and then levels off to the limiting case of $D = \infty$, which has a reactive state yield of 0.82. The parameters are $a_f = 1$ Å, $R_f = 12$ Å, $\tau = 20$ ns, $R_m = 9$ Å, $d = 7.2$ Å, and $C = 0.3$ M.

where ϕ_{ex}, the relative fluorescence yield, is

$$\phi_{ex} = \frac{1}{\tau}\int_0^\infty \langle P_{ex}(t)\rangle dt. \tag{68}$$

ϕ_{re} shows the total number of ions formed for a given set of forward electron-transfer parameters and diffusion constants irrespective of whether they back transfer to the ground state or escape. The reactive state yield can also be obtained using the reactive state probability function given by Eq. (59). Equation (59) in the limit that the back transfer rate goes to zero and time goes to infinity gives Eq. (67). The parameters used to calculate Fig. 3 were $a_f = 1$ Å, $R_f = 12$ Å, $\tau = 20$ ns, $C = 0.3$ M, $d = 7.2$ Å, and $R_m = 9.0$ Å. The diffusion constants used are shown Fig. 3. As can be seen, as the diffusion constant increases the number of ions formed increases. This happens because diffusion brings acceptors that were too far away for electron transfer closer to the donor, effectively increasing the number of acceptors with which the donor interacts. The increase in the yield is greatest for small diffusion constants then levels off and approaches the infinite diffusion constant result at large diffusion constants.

The reactive state probability is plotted as a function of time and diffusion constant for each case defined in Sec. I in Fig. 4. Following $t = 0$, forward electron transfer creates reactive pairs, and back electron transfer is destroying them. At $D = 0$ and $D = \infty$, the three cases give the same results. In solid solution the particles are fixed. In the case of infinite diffusion constant the particle motion is so fast that the reactive state once created moves far away from the donor and does not back transfer. If the recombination were not geminate, and there was a constant background concentration of nongeminate acceptor molecules for the reactive state, then the three cases would be different and the probability would decay.

For diffusion constants of 1, 10, and 100 Å^2/ns, the three cases are different. $V(R)$ is Coulombic and the relative permittivity (ϵ_r) used for Fig. 6 is 78.5 (water). All calcula-

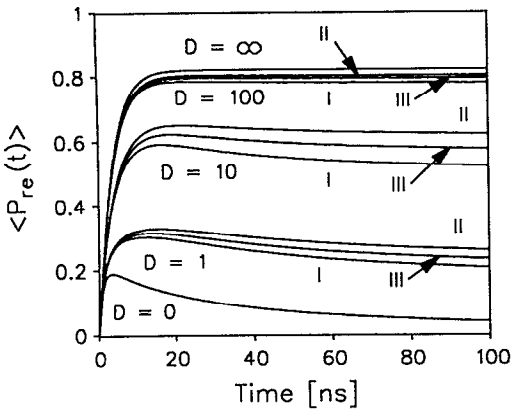

FIG. 4. Reactive state probability as a function of time. The back transfer parameters are equal to the forward transfer parameters used in Fig. 3. Case I has an attractive Coulomb potential, case II has a repulsive Coulomb potential, and case III has no potential. $\epsilon_r = 78.5$, the value for water. As the diffusion constant increases so does the reactive state probability.

tions were performed using a temperature of 298 K. In the figures, case I has an attractive potential, case II has a repulsive potential, and case III has no potential between the donor and the acceptor in the reactive state. The forward transfer rate is equal to the back transfer rate (the parameters are in the caption of Fig. 3). Faster back transfer results in a lower reactive state probability at any time. The repulsive case gives the highest reactive state probability while the attractive case gives the least. The differences among the curves are not great because of the high relative permittivity used in the calculation (see the following).

In Fig. 5 the reactive state probability is plotted as a function of time and relative permittivity (ϵ_r). The parameters are the same as in Fig. 3, except $D = 10$ Å^2/ns for all curves. The ϵ_r's used are $\epsilon_r = 1$ for free space, $\epsilon_r = 6.02$ for ethyl acetate, and $\epsilon_r = 24.3$ for ethanol. The neutral case is given in Fig. 5 and lies between the attractive and repulsive cases and is independent of ϵ_r. For decreasing ϵ_r, the reactive state probability decreases for the attractive case and increases with the repulsive case. The Coulombic force between a pair of ions is greatest in free space and decreases with increasing ϵ_r.

The attractive case seems to be more dramatically affected by decreasing ϵ_r than the repulsive case. When the ions are repulsed their survival probability increases and the reactive state probability also increases but it cannot increase any faster then the rate of ion formation, which is determined by the forward transfer parameters and the diffusion constant. When the ions are attracted, their survival probability will decrease because the back transfer sink function is largest at smaller separations.

In Fig. 6 the reactive state survival fraction, $f_s(t)$, is plotted as a function of diffusion constant. The survival fraction is defined as the fraction of all reactive states formed that still survive at a time t. The reactive state probability is obtained from Eq. (59). The total number of reactive states formed by a time t is given by Eq. (59) in the limit that the back transfer rate goes to zero, $\langle P_{re}(t)\rangle_{k_b=0}$. The survival fraction is then given by

$$f_s(t) = \frac{\langle P_{re}(t)\rangle}{\langle P_{re}(t)\rangle_{k_b=0}}. \tag{69}$$

In the limit of long time this would give the reactive state escape probability. This is the fraction of all reactive states that did not undergo geminate recombination. In Fig. 6 the survival fraction at $t = 100$ ns is plotted as a function of diffusion constant for the three cases. In all three cases the survival fraction increases rapidly between zero and 20 Å^2/ns. At larger diffusion constants the survival fraction increases more slowly. As was noted in Fig. 3 the reactive state yield also increases significantly in this range. Thus, not only are there more reactive states generated with larger diffusion constants but a greater percentage of them survive. Case I, which has the attractive potential, has the smallest

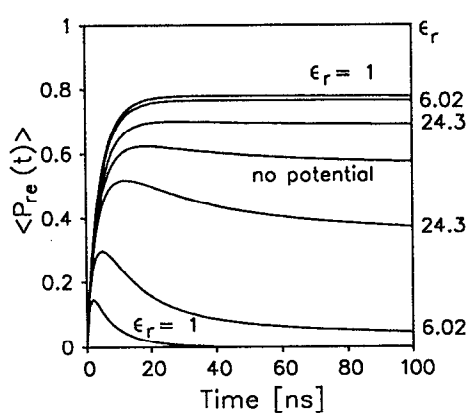

FIG. 5. Reactive state probability as a function of time and relative permittivity (ϵ_r). The parameters are the same used in Fig. 3 except $D = 10$ Å^2/ns and the relative permittivities are given in the figure. $\epsilon_r = 1$ is the value for free space, $\epsilon_r = 6.02$ is the value for ethyl acetate, and $\epsilon_r = 24.3$ is the value for ethanol at 298 K. The curves above the no potential case have a repulsive Coulomb potential while the curves below have an attractive Coulomb potential.

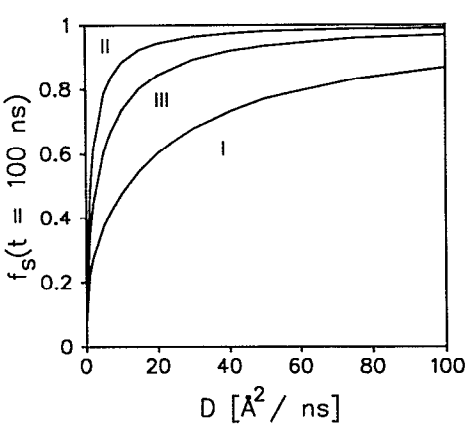

FIG. 6. Reactive state survival fraction at $t = 100$ ns as a function of diffusion constant. The parameters are the same used in Fig. 3 with $\epsilon_r = 24.3$ and with the cases defined in the text. As the diffusion constant increases the survival fraction increases.

survival fraction while case II, which has the repulsive potential, has the largest survival fraction. The relative permittivity used in Fig. 6 was $\epsilon_r = 24.3$ (ethanol). The other parameters are in the caption of Fig. 6. At higher relative permittivities, the three cases would be closer while at smaller relative permittivities they would be further apart.

In Fig. 7 the survival fraction is plotted as a function of relative permittivity for a diffusion constant of $D = 10$ Å^2/ns with the other parameters the same as Fig. 6. As can be seen the no potential case (III) is independent of ϵ_r and lies between the repulsive (II) and attractive (I) cases. At sufficiently large relative permittivities, the three cases should converge to the same result. As seen in Fig. 7 the three cases get closer together and more symmetric about the no potential case at large relative permittivities. At smaller relative permittivities the cases become quite different. For the attractive case, the survival fraction falls almost to zero while the survival fraction for the repulsive case goes almost to one.

The reactive state distribution function $P_{re}(R,t)$, given by Eq. (58), is plotted in Figs. 8–10 as a function of the donor–acceptor separation R. In the figures $P_{re}(R,t)$ is multiplied by $4\pi CR^2 dR$, where we have set $dR = 1$. This gives the probability that the donor and acceptor molecules in the reactive state have the separation R at a time t. This type of figure provides insight into the relative positions of the reactive pair. The total reactive state probabilities discussed are the integrals of curves like those in Figs. 8–10 integrated over R. In Fig. 8, the reactive state distribution function is plotted as a function of diffusion constant for the no potential case (III) at a time of 1 ns. The diffusion constants range from 0 to 100 Å^2/ns. The other parameters are given in the caption of Fig. 8. As the diffusion constant gets larger the height of the distribution falls and moves to longer distances and the width of the distribution gets wider. The reactive state probability at short distances gets smaller with increasing diffusion constant, and there is a greater probability for the reactive state pair to separate before it back transfers.

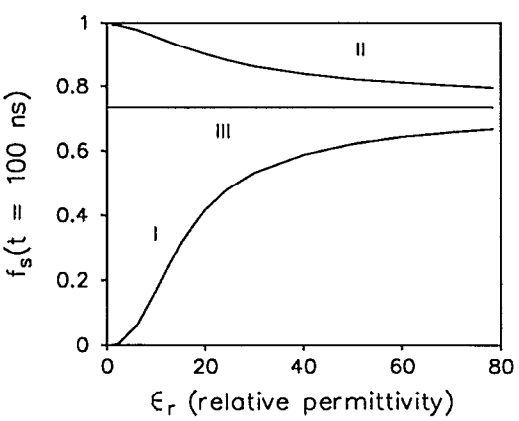

FIG. 7. Reactive state survival fraction at $t = 100$ ns as a function of relative permittivity. The parameters are the the same as in Fig. 3 except $D = 10$ Å^2/ns. As the relative permittivity increases the three cases get closer together while at small relative permittivities they diverge.

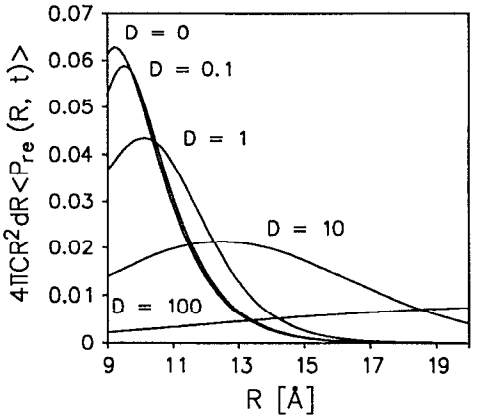

FIG. 8. Reactive state distribution function as a function of distance and diffusion constant. This is for the no potential case (III) at time $t = 1$ ns. Diffusion constants (Å^2/ns) are given in the figure. The other parameters are the same as in Fig. 3. As the diffusion constant increases the distribution moves to longer distances and gets wider.

Figure 9 gives the reactive state distribution function as a function of the relative permittivities for the attractive case (I). The diffusion constant is $D = 10$ Å^2/ns, and the time is 1 ns. The other parameters are given in the caption of Fig. 9. At high relative permittivities, the distribution looks like that of the neutral case. A comparison of curve D ($\epsilon_r = 78.5$) in Fig. 9 with curve $D = 10$ Å^2/ns in Fig. 8 shows that they are similar in shape and magnitude. As the relative permittivity decreases the interaction potential increases between the ions in the reactive state and pulls the pairs closer together. This has the effect of increasing the magnitude of the reactive state distribution function at short distances while depleting it at large distances. Since the ions are closer the probability for back transfer is greater, thus the total reactive state probability is less. This is demonstrated in

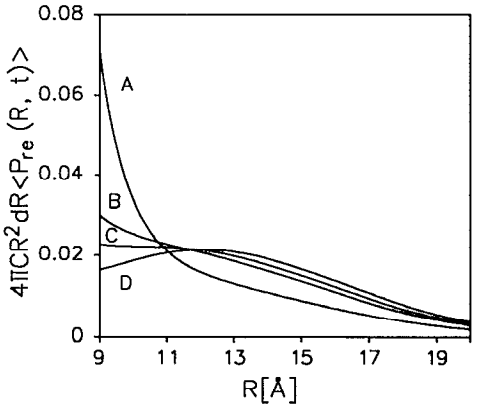

FIG. 9. Reactive state distribution function as a function of distance and relative permittivity ϵ_r. This is for the attractive case (I) for $D = 10$ Å^2/ns and $t = 1$ ns. The curves labeled A, B, C, and D correspond to relative permittivities 6.02, 15, 24.3, and 78.5, respectively. The other parameters are the same as in Fig. 3. The smaller the relative permittivity the greater is the reactive state probability at shorter distances while it is less at larger distances.

Figs. 5 and 7, which display the reactive state probability and survival fraction, respectively, as a function of relative permittivity.

Figure 10 gives the reactive state distribution function as a function of distance and relative permittivity for the repulsive case (II). The diffusion constant is $D = 10$ Å^2/ns, and the time is 1 ns. The other parameters are given in the caption of Fig. 10. As in Fig. 9, the case at high ϵ_r (D) is similar to the case with no potential given by curve $D = 10$ Å^2/ns in Fig. 8. Relative to Fig. 9 the distribution has been pushed out because of the repulsive potential and the areas under the curves are greater. Since the ions in the reactive state are pushed further apart, the probability for back transfer is less than the neutral or repulsive cases. This results in a higher reactive state probability and a larger survival fraction.

In Fig. 11, the reactive state probability (the total probability unlike Figs. 8–10 that are functions of R), given by Eq. (59), is plotted for the full theory presented here and two approximate models for the reactive state survival probability, $S_{re}(t|R_0)$, for the no potential case (III). In all curves, the excited state survival probability, $S_{ex}(t,|R_0)$, and the excited state probability, $\langle P_{ex}(t),\rangle$ were calculated using Eqs. (24) and (42), respectively. That is, the detailed method for the forward transfer was employed rather than the more approximate models discussed in relation to Fig. 2. The parameters used to calculate these are given in the caption of Fig. 11. In curve A, the Collins and Kimball model is used to calculate $S_{re}(t|R_0)$ for Eq. (59) and is given by[26]

$$S_{re}(t|R_0) = 1 - \frac{R_m}{R_0}\left(\frac{k}{k + 4\pi R_m D}\right)\left[\operatorname{erfc}\left(\frac{R_0 - R_m}{\sqrt{4Dt}}\right) - \exp[\alpha^2 Dt + \alpha(R_0 - R_m)] \times \operatorname{erfc}\left(\alpha\sqrt{Dt} + \frac{R_0 - R_m}{\sqrt{4Dt}}\right)\right]. \quad (70)$$

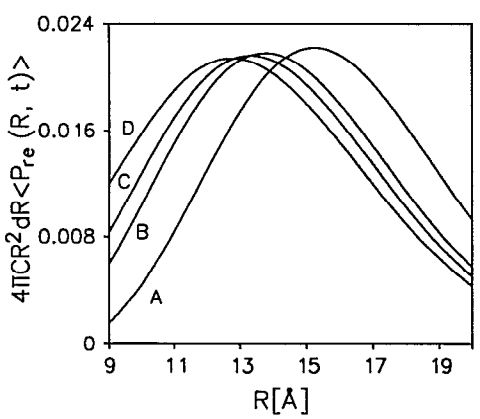

FIG. 10. The reactive state distribution function as a function of distance and relative permittivity ϵ_r. This is for the repulsive case (II) for $D = 10$ Å^2/ns and $t = 1$ ns. The curves labeled A, B, C, and D correspond to relative permittivities 6.02, 15, 24.3, and 78.5, respectively. The other parameters are the same as in Fig. 3. For smaller relative permittivities, the reactive state probability is less at shorter distances while it is greater at larger distances.

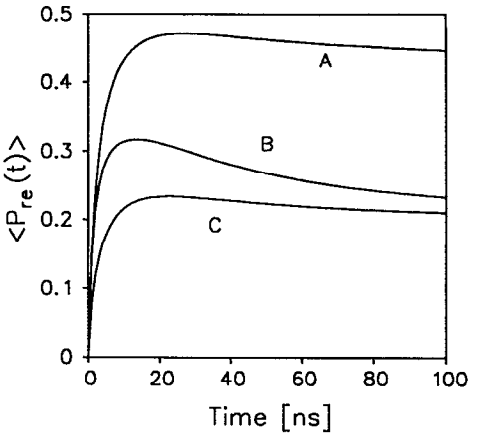

FIG. 11. The reactive state probability as a function of time for various models for the reactive state survival probability, $S_{re}(t|R_0)$ for the no potential case (III). The rate of reactive state formation is given by the model developed here. Curve A uses the Collins and Kimball model for $S_{re}(t|R_0)$, curve B has $S_{re}(t|R_0)$ given by Eq. (27), and curve C uses the Smoluchowski model for $S_{re}(t|R_0)$. The parameters are the same as used in Fig. 3 except $D = 1.0$ Å^2/ns and $k = 1275$ Å^3/ns for the Collins and Kimball model and was calculated using Eq. (60). The Smoluchowski model underestimates the reactive state probability while the Collins and Kimball model overestimates it.

It is necessary to choose a value for k to be consistent with the detailed theory; k is given by Eq. (62), which for the parameters used here is $k = 1275$ Å^3/ns. Curve B uses the solution to Eq. (27), which has a distance dependent sink function, and curve C uses the Smoluchowski model, which is given by the following equation:[26]

$$S_{re}(t|R_0) = 1 - \frac{R_m}{R_0}\operatorname{erfc}\left(\frac{R_0 - R_m}{\sqrt{4Dt}}\right). \quad (71)$$

As can be seen the Smoluchowski model underestimates the reactive state probability, while curve A, the Collins and Kimball, overestimates it. It must be pointed out that the Collins and Kimball model, although further from curve B than the Smoluchowski model, is better at higher diffusion constants. As the diffusion constant gets smaller the Collins and Kimball model will increasingly underestimate the amount of back electron transfer. This is because all the electron transfer happens at contact in the Collins and Kimball model, while the model presented here allows transfer at separations other than contact. Moreover, the disagreement between the curves in Fig. 11 would be larger had the rate of ion formation been calculated using the Smoluchowski model in curve C, and the Collins and Kimball model in curve A. This was demonstrated by the attempt to fit the curves in Fig. 2 with the Collins and Kimball, and Smoluchowski models in Sec. III A. Furthermore, if data taken as a function of diffusion constant is fit with either the Collins and Kimball or Smoluchowski models, the electron transfer parameters will not be consistent. It is interesting to note, however, that the Collins and Kimball model is better at short time while the Smoluchoski model is better at long time.

C. Experimental observables

Using the state probabilities calculated earlier, experimental observables can be calculated. It is possible to moniter the ground-state population using a ground-state recovery experiment such as a pump–probe experiment. It will be assumed that at the probe wavelength there are no other absorbing states besides the donor ground state and that there is no stimulated emission.[52] The pump–probe observable for the ground state is then given by[7]

$$S(t) = A\,[1 - \langle P_{gr}(t)\rangle], \tag{72}$$

where A is a constant. After substituting Eq. (60) for the ground-state probability one obtains

$$S(t) = A\,[\langle P_{ex}(t)\rangle + \langle P_{re}(t)\rangle]. \tag{73}$$

This has been calculated for a variety of diffusion constants for the no potential case (III) in Fig. 12. The other parameters are in the caption. As can be seen, as the diffusion constant increases the extent of decay decreases, and for infinite diffusion the decay levels off to a constant. At short time, the signal is dominated by the fall in the excited-state population. This can be seen for the same parameters in Fig. 2 for $C = 0.3$ M. At long time, the excited-state population has decayed to zero for the larger diffusion constants and the observable is dominated by the reactive state probability. It is possible to measure the reactive state survival fraction by measuring the pump–probe observable out far enough in time that the excited state has decayed to zero. At this time the magnitude of the observable is the reactive state probability at that time. The total number of reactive states formed can be obtained from a fluorescence yield measurement. From Eq. (67) the total ion yield can be obtained from the fluorescence yield. To obtain the survival fraction the long-time value of the observable is divided by ion yield as in Eq. (73) (for large t).

IV. CONCLUDING REMARKS

In this work a model has been presented which accounts for the effects of diffusion on photoinduced electron transfer with geminate back transfer for transfer rates that are distance dependent. Both donor–acceptor and acceptor–acceptor excluded volume have been taken into account, as well as the effect of a Coulomb interaction potential between the donors and the acceptors. Comparisons to other theories were made, and we have shown where they might be applicable and where the theories differ. A wide range of diffusion constants from 0 to ∞ were used. At intermediate and small diffusion constants the Smoluchowski, and Collins and Kimball results do not yield consistent electron-transfer parameters; therefore the model with a distance dependent rate must be used. The inclusion of an interaction potential has enabled us to compare three different cases for the reactive state. When there is no interaction potential there is free diffusion, and the dynamics are completely determined by the electron-transfer parameters and the diffusion constant. For the attractive and repulsive cases, as the relative permittivity gets smaller the interaction potential gets larger and so does the effect on the reactive state population. The attractive potential will give a smaller reactive state yield and survival fraction while the repulsive potential will give a larger reactive state yield and survival fraction. The reactive state yield is the total number of ions formed and the survival fraction is the fraction of the reactive state population still in existence at a time t. In the long-time limit (time long compared to the electron transfer and diffusion time scale) the reactive state survival fraction becomes the reactive state escape probability. It has also been shown how these quantities can be related to experimental data.

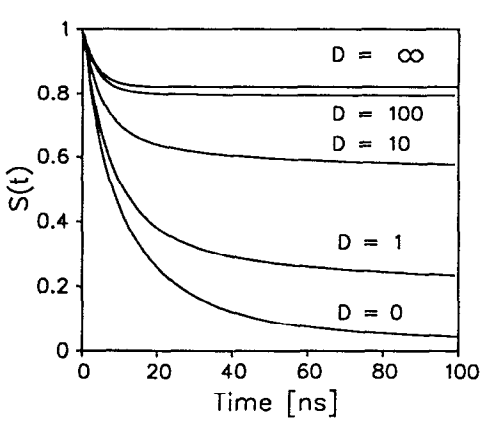

FIG. 12. The pump–probe observable as a function of time and diffusion constant for the no potential case (III). The parameters are the same as those used in Fig. 3. As the diffusion constant increases the observable decays more slowly.

ACKNOWLEDGMENT

This work is supported by the Department of Energy, Office of Basic Energy Sciences (Grant No. DE-FG03-84ER13251). Computing equipment was provided by the National Science Foundation Computing Grant (No. CHE 88-21737). We would also like to thank M. Tachiya, A. Szabo, and N. Agmon for helpful correspondence.

[1] T. Guarr and G. McLendon, Coord. Chem. Rev. **68**, 1 (1985).
[2] R. G. Gordon, J. Chem. Phys. **44**, 1830 (1965).
[3] G. E. Uhlenbeck and L. S. Ornstein, Phys. Rev. **36**, 823 (1930).
[4] B. Cichocki and B. U. Felderhof, J. Chem. Phys. 1988, **89**, 1049 (1988).
[5] M. V. Z. Smoluchowski, Phys. Chem. **92**, 129 (1918).
[6] J. Crank, *The Mathematics Of Diffusion* (Oxford University, London, 1956).
[7] Y. Lin, R. C. Dorfman, and M. D. Fayer, J. Chem. Phys. **90**, 159 (1989).
[8] R. C. Dorfman, Y. Lin, M. D. Fayer, J. Phys. Chem. **93**, 6388 (1989).
[9] P. W. Atkins, *Physical Chemistry* (Freeman, New York, 1986).
[10] *Direct Energy Conversion*, edited by George W. Sutton (McGraw-Hill, New York, 1966).
[11] *Photo-Electrochemical Solar Cells*, edited by K. S. V. Santhanam and M. Sharon (Elsevier, New York, 1988).
[12] L. Onsager, Phys. Rev. **54**, 554 (1938).
[13] S. Chandrasekar, Rev. Mod. Phys. **15**, 1 (1943).
[14] P. Debeye, J. Electrochem. Soc. **82**, 265 (1942).
[15] M. M. Agrest, S. F. Kilin, M. M. Rikenglaz, and I. M. Rozman, Opt. Spectrosc. **27**, 514 (1969).
[16] J. Kusba and B. Sipp, Chem. Phys. **124**, 223 (1988).
[17] B. Sipp and R. Voltz, J. Chem. Phys. **79**, 434 (1983).
[18] B. Sipp and R. Voltz, J. Chem. Phys. **83**, 157 (1985)
[19] I. Z. Steinberg, and E. Katchalski, J. Chem. Phys. **48**, 2404 (1968).
[20] M. Yokota and O. Tanimoto, J. Phys. Soc. Jpn. **22**, 779 (1967).

[21] K. Allinger and A. Blumen, J. Chem. Phys. **72**, 4608 (1980).
[22] K. Allinger and A. Blumen, J. Chem. Phys. **75**, 2762 (1981).
[23] J. Baumann and M. D. Fayer, J. Phys. Chem. **85**, 4087 (1986).
[24] D. D. Eads, B. G. Dismer, and G. R. J. Fleming, Chem. Phys. **93**, 1136 (1990).
[25] L. Song, R. C. Dorfman, S. F. Swallen, and M. D. Fayer, J. Phys. Chem. **95**, 3454 (1991).
[26] S. A. Rice, *Diffusion-Limited Reactions* (Elsevier, Amsterdam, 1985).
[27] P. Chatterjee, K. Kamioka, J. D. Batteas, and S. E. Webber, J. Phys. Chem. **95**, 960 (1991).
[28] J. Najbar, Chem. Phys. **120**, 367 (1988).
[29] Z. Schulten and K. Schulten, J. Chem. Phys. **66**, 4616 (1977).
[30] H. J. Werner, Z. Schulten, and K. Schulten, J. Chem. Phys. **67**, 646 (1977).
[31] J. Najbar and A. M. Turek, Chem. Phys. **142**, 35 (1990).
[32] M. Tachiya, Radiat. Phys. Chem. **21**, 167 (1983).
[33] N. Agmon and A. Szabo, J. Chem. Phys. **92**, 5270 (1990).
[34] A. Szabo, R. Zwanzig, and N. Agmon, Phys. Rev. Lett. **61**, 2496 (1988).
[35] S. Rabinovich and N. Agmon, Chem. Phys. **148**, 11 (1990).
[36] N. J. Agmon, Chem. Phys. **90**, 3765 (1989).
[37] M. S. Mikhelashvili, J. Feitelson, and M. Dodu, Chem. Phys. Lett. **171**, 575 (1990).
[38] M. S. Mikhelashvili and M. Dodu, Phys. Lett. A **146**, 436 (1990).
[39] R. C. Dorfman, M. Tachiya, and M. D. Fayer, Chem. Phys. Lett. **179**, 152 (1991).
[40] O. A. Karim, A. D. J. Haymet, M. J. Banet, and J. D. Simon, J. Phys. Chem. **92**, 3391 (1988).
[41] M. Sparglione and S. Mukamel, J. Chem. Phys. **88**, 3263 (1988).
[42] I. Rips, J. Klafter, and J. Jortner, J. Chem. Phys. **88**, 3246 (1988).
[43] S. Su and J. D. Simon, J. Phys. Chem. **93**, 753 (1989).
[44] A. Chandra and B. Bagchi, J. Chem. Phys. **90**, 1832 (1989).
[45] D. Y. Chu and J. K. Thomas, Macromolecules, **23**, 2217 (1990).
[46] M. Inokuti, and F. Hirayama, J. Chem. Phys. **28**, 87 (1965).
[47] A. Blumen and J. Manz, J. Chem. Phys. **71**, 4694 (1979).
[48] A. Blumen, J. Chem. Phys. **72**, 1632 (1980).
[49] J. Najbar, R. C. Dorfman, and M. D. Fayer, J. Chem. Phys. **94**, 1081 (1991).
[50] W. H. Press, B. P. Flannery, S. A. Teukolsky, and W. T. Vetterling, *Numerical Recipes In C* (Cambridge University, Cambridge, 1988).
[51] E. Pines, D. Huppert, and N. Agmon, J. Chem. Phys. **88**, 5620 (1988).
[52] L. Song and M. D. Fayer, J. Lumin. **50**, 75 (1991).